Dalton Transactions

Accepted Manuscript

ROYAL SOCIETY OF CHEMISTRY

www.rsc.org/dalton

Dalton Transactions

RSCPublishing

ARTICLE

Atomic layer deposition of quaternary oxide (La,Sr)$CoO_{3-\delta}$ thin films

Cite this: DOI: 10.1039/x0xx00000x

E. Ahvenniemi[a], M. Matvejeff[a] and M. Karppinen[a,*]

Received ooth January 2015,
Accepted ooth January 2015

DOI: 10.1039/x0xx00000x

www.rsc.org/

A novel atomic layer deposition (ALD) process was developed for fabricating quaternary cobalt oxide ($La_{1-x}Sr_x$)$CoO_{3-\delta}$ thin films having the eye on future applications of such films in *e.g.* solid oxide fuel cell cathodes, oxygen separation membranes or thermocouples. The deposition parameters and the conditions of a subsequent annealing step were systematically investigated, and using the thus optimized parameters the cation stoichiometry in the films could be accurately tuned. The most detailed study was conducted for x = 0.7, *i.e.* the composition with the highest application potential within the ($La_{1-x}Sr_x$)$CoO_{3-\delta}$ system.

Introduction

Most of the state-of-the-art intermediate temperature solid oxide fuel cell (IT-SOFC) cathode materials are ABO_3 perovskite mixed ionic-electronic conductors (MIEC); they moreover need to be highly porous and participate in both the oxygen reduction reaction (ORR) and the oxide ion transport.[1,2] In the typical high-performance MIEC material, (La,Sr)(Co,Fe)$O_{3-\delta}$, the proper La:Sr ratio at the A-site ensures the high electrical conductivity and the Fe-for-Co substitution at the B-site is used to tune the thermal expansion coefficient (TEC) to match that of the substrate material. The latter circumstance is important as it diminishes the harmful thermal stresses when the fuel cell temperature is cycled, significantly prolonging the cell´s lifetime. Another efficient way to enhance the performance of an IT-SOFC cathode is to reduce the layer thickness as was demonstrated by Prestat *et al.*[3] for ($La_{0.52}Sr_{0.48}$)($Co_{0.18}Fe_{0.82}$)$O_{3-\delta}$ where the polarization resistance dropped by 1-1.5 orders of magnitude when the bulk diffusion pathway was eliminated by reducing the film thickness from 766 nm to 16 nm. Other studies have revealed that the ORR rather than the oxide ion conductivity in the bulk is the rate limiting step.[4-6] In other words, a thin and porous cathode would significantly increase the IT-SOFC performance and facilitate the operation in the intermediate temperature range, enabling decent start-up times and increased life-time of the critical components. Unfortunately, the cobalt oxide cathodes often exhibit very high values for TEC (14–21 $ppmK^{-1}$) that are incompatible with the most commonly employed electrolyte materials, such as Y-stabilized zirconia (10.5 $ppmK^{-1}$), Gd-doped ceria (13.5 $ppmK^{-1}$) and (La,Sr)(Ga,Mg)O_3 (2020) (11.1 $ppmK^{-1}$).[2]

For the ($La_{1-x}Sr_x$)$CoO_{3-\delta}$ perovskite system the important material properties can be readily tuned with the adjustment of the strontium content. The optimal Sr substitution level x is between 0.3–0.7, as the phase exhibits a metal-insulator transition around x = 0.25.[7] According to Iwasaki *et al.*[8] poly-crystalline samples exhibit metallic conductivity between 100–1000 K for x > 0.3, while according to Kozuka *et al.*[9] electrical conductivity and carrier concentration are the highest for x = 0.2–0.8 (rhombohedral phase). The structure changes to cubic symmetry at high values of x, eventually leading to the formation of the insulating brownmillerite phase, $SrCoO_{2.5}$.

There are only a few thin film deposition techniques capable of industrial scale operation and deposition on micro- or nanostructured substrates without adverse shadowing effects. The atomic layer deposition (ALD) technique is based on sequential gas-to-surface reactions and can be applied even on high-aspect-ratio surfaces and nanoparticles.[10] Even though the focus in ALD research has for a long time been on binary oxide compounds, *e.g.* HfO_2, Al_2O_3, ZnO and TiO_2, driven mainly by the interests of IC and MEMS industries, the technique can be used to deposit ternary and quaternary oxides as well, and in recent years the focus has been slowly extended to cover also

the more complex high-performance materials for a variety of future technologies, such as thermoelectrics and spintronics.[11,12]

For possible SOFC application not only thin films of Y-stabilized zirconia,[13,14] Gd-doped ceria[15] and some ternary oxide materials[16-19] have been fabricated by ALD, but also some quaternary perovskite oxides, *i.e.* (La,Ca)$MnO_{3-\delta}$,[20] (La,Sr)$FeO_{3-\delta}$[21] and (La,Sr)$MnO_{3-\delta}$[22]. Among the quaternary perovskite oxides, the ($La_{1-x}Sr_x$)$CoO_{3-\delta}$ system possesses the best oxide ion transport properties.[23] The ($La_{1-x}Sr_x$)$CoO_{3-\delta}$ phase can also be used as an electrode to replace Pt and Ag due to its high electrical conductivity and temperature resiliency, or as a gas permeable membrane,[9,24–26] thus making it a highly interesting and versatile material candidate for MIEC and oxygen separation processes.[23,27,28] To enhance its promising practical properties, the material should be able to be processed with a method where nanostructuring, *i.e.* increasing the active surface area, is possible and the control of the cation stoichiometry is precise. The ALD method can address these criteria, even though introducing more cations often makes the process difficult to optimize. In this paper, a novel ALD process is presented to manufacture high-quality ($La_{1-x}Sr_x$)$CoO_{3-\delta}$ thin films with a readily tunable composition *x*.

Experimental

Thin films of (La,Sr)$CoO_{3-\delta}$ were successfully grown in a commercial ALD reactor (F-120, ASM Microchemistry Ltd.) using $La(thd)_3$ (thd: 2,2,6,6-tetramethyl-3,5-heptanedione), $Sr(thd)_2$, $Co(acac)_3$ (acac: acetylacetonate) as metal precursors and ozone as the oxygen source. The $La(thd)_3$ and $Sr(thd)_2$ precursors were prepared in-house,[29] while a commercial source was used for the $Co(acac)_3$ precursor (Sigma, CAS: 21679-46-9, 99.99%). An external ozone generator (Fischer Model 502) was used to generate 10% O_3 gas. The temperatures used to sublimate the solid metal precursors were fixed at 175, 200 and 142 °C for $La(thd)_3$, $Sr(thd)_2$ and $Co(acac)_3$, respectively, based on our preliminary data from thermogravimetric analysis (TG; Perkin-Elmer TGA 7) and sublimation rates in the F-120 reactor. Thermogravimetric analyses revealed a complete sublimation with no significant residue for all the precursors. Nitrogen (99.999 %, 300 sccm, Schmidlin UHPN 3000N generator) was used as the carrier and purge gas in the depositions with the background pressure of *ca*. 2–3 mbar (1.5–2 Torr).

All the depositions were performed on silicon (p-type, Si(100), Okmetic Ltd.) and borosilicate (Duran Group Ltd.) substrates. Deposition temperature was optimized within the limits defined by the $Sr(thd)_2$ sublimation temperature (*ca*. 200 °C) and the loss of self-terminating growth mode due to the thermal decomposition of precursors above 330 °C. For ternary and quaternary oxide thin films, it is common that ALD at these temperatures yields amorphous films; in a present case too, a heat treatment was required for crystallizing the products. This post-deposition annealing was performed using a 15 min heating in a rapid thermal annealing furnace (RTA; PEO 601, ATV Technologie GmbH) at temperatures between 500–1000 °C under typical SOFC cathode operation conditions, *i.e.* using 5.0 O_2 or air-gas (20 % 5.0 O_2 + 80 % 5.0 N_2) at the flow rate of 200 l/h. The heating and cooling rates were set to 20 °C/min and 25 °C/min, respectively.

Metal composition for the as-deposited thin films was calculated from X-ray fluorescence spectroscopy (XRF; PANalytical Axios^{mAX} with a Rh tube, 3 kW model) data. For selected samples, the XRF result was verified with inductively-coupled-plasma optical-emission spectrometry (ICP-OES; Perkin Elmer ICP-OES, 7100 DV) measurements, by dissolving the thin film into conc. HCl, and then diluting the acid to *ca*. 1 M before the measurement. Structure of the post-deposition annealed films was examined by grazing incidence X-ray diffraction (GIXRD; PANalytical model X'Pert PRO diffractometer, Cu Kα radiation, λ = 1.5405980 Å) and the film thickness was determined with X-ray reflectivity (XRR; PANalytical model X'Pert PRO diffractometer, Cu Kα radiation). The film thicknesses were calculated with both the direct calculation method and the Fourier method, using the averages of obtained values.

Results and discussion

The three metal precursors, $La(thd)_3$, $Sr(thd)_2$ and $Co(acac)_3$, were first tested separately to search for the optimal pulsing lengths for the precursor and the ozone gas. The test depositions were carried out at 290 °C, selected for being a typical deposition temperature in case of β-diketonate precursors and for yielding visually non-gradient films over the entire substrate surface. At first, the O_3 pulse length was fixed to 3.0 s (N_2 purge length after the O_3 pulse was fixed to 2.5 s) and the metal precursor pulse length was varied from 0.5 to 6.0 s (N_2 purge length after the precursor pulse was fixed to 1.5 s). In Fig. 1 we plot the growth-per-cycle (GPC) values for the binary oxides against the metal precursor pulse length, calculated from the film thicknesses immediately after the deposition to avoid possible later thickness variations induced by atmospheric moisture. It is seen that the GPC values saturate at *ca*. 1.5-2.0 s of pulse length for each metal precursor. Subsequently, test depositions were carried out where the metal precursor pulse length was kept at 1.5 s (with 1.5 s N_2 purge), while the O_3 pulse length was varied from 1.5 to 6 s (N_2 purge length was kept at 2.5 s). Purge lengths were tested for precursors and ozone with 1.5, 2.5 and 3.5 s, and 2.5, 3.5 and 4.5 s long pulses, respectively, and no effects were seen on the film thicknesses. Using these results, the metal precursor pulse length was chosen to be 2.0 s for all three precursors to ensure a good surface coverage; the O_3 pulse length was set to 3.0 s for all the metal precursors, to be long enough for a complete oxygenation of the film, but short enough to avoid possible etching of the film. The N_2 purges after the precursor and ozone pulses were kept at 1.5 s and 2.5 s, respectively. From here on the pulse lengths are not mentioned anymore, as they were kept fixed.

From Fig. 1, it can be seen that the saturated GPC value is heavily dependent on the number and size of the remaining

ligands, where the least amount of ligands is preferred over the size, giving the growth rate order of $Sr(thd)_2$ > $Co(acac)_3$ > $La(thd)_3$. This observation is in line with the reaction mechanism in which the precursor molecule detaches one of its ligands as it is adsorbed to the surface, *e.g.* $Sr(thd)_2$ is adsorbed to the surface as $Sr(thd)^-$, and thus the Sr carbonate film grows faster since $Sr(thd)^-$ takes less space than $La(thd)^{2-}$ or $Co(acac)^{2-}$ on the surface. In a similar way, the adsorbed $Co(acac)^{2-}$ is smaller than $La(thd)^{2-}$, thus having more space to promote the faster film growth.

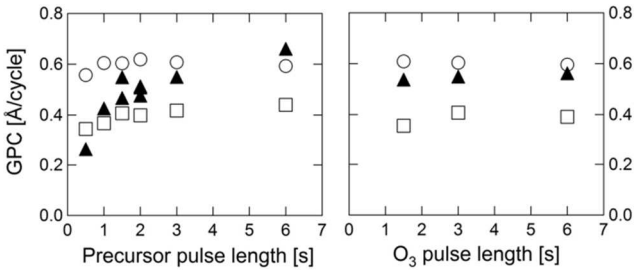

Fig. 1 Left: Growth-per-cycle (GPC) *vs*. precursor pulse length for $Sr(thd)_2$ (○), $Co(acac)_3$ (▲) and $La(thd)_3$ (□). Right: GPC *vs*. O_3 pulse length. Each precursor was tested individually with 1000 deposition cycles.

The so-called ALD window, *i.e.* the deposition temperature range where the GPC value remains constant, was searched for the quaternary La-Sr-Co-O system between 230–330 °C by depositing in total 300 supercycles of each metal precursor in the sequence, [$La(thd)_3$ → $Co(acac)_3$ → $Sr(thd)_2$ → $Co(acac)_3$], and monitoring the film thickness *vs*. deposition temperature. From Fig. 2, the ALD window is estimated around 250–310 °C, where 290 °C was chosen for the further depositions. This wide ALD window for a quaternary process is quite unusual, as usually the ALD window becomes distinctly narrow even for ternary processes.

Let us then discuss the possibility to control the metal composition in our quaternary La-Sr-Co-O films by changing the relative numbers of the individual metal precursor cycles (consisting of the metal precursor pulse and the ozone pulse). In these depositions, the so-called supercycle, [a × P1 → b × P2 → c × P3], was repeated d times, where P1, P2 and P3 stand for the three metal precursor pulses (*plus* subsequent ozone pulses), and a, b or c indicate the number of repetitions applied for the corresponding precursor pulse in one supercycle. Here we changed the supercycle parameters, a, b and c, such that two out of them were kept fixed, while varying one of them. For

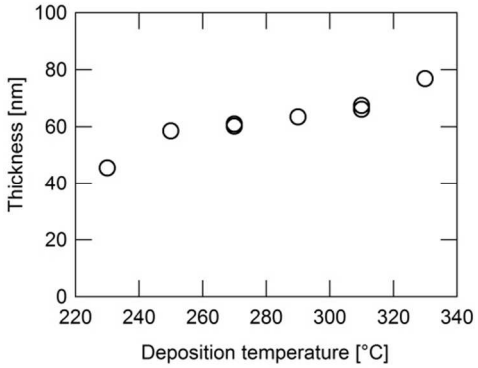

Fig. 2 Film thickness vs. deposition temperature for the growth of ternary La-Sr-Co-O films, where the cation pulse sequence was 300 × [1 × $Sr(thd)_2$ → 1 × $Co(acac)_3$ → 1 × $La(thd)_3$ → 1 × $Co(acac)_3$].

example, in Fig. 3 (left image), the repetitions of $Sr(thd)_2$ and $Co(acac)_3$ precursor cycles in one supercycle were kept fixed to 1 and 2, respectively, while the number of $La(thd)_3$ cycles was varied from 2 to 8, and the resultant La-to-Co ratio in the films was determined by XRF (and confirmed by ICP-OES). Similar deposition schemes were carried out for strontium and cobalt as well, with 3 cycles for La and 2 for Co, and 3 for La and 2 for Sr, respectively. The La and Co contents were found to increase straightforwardly with the number of respective cycles, while the proportion of Sr was showing a slight saturation at higher repetitions. Based on the data from Fig. 3, we selected the supercycle [3 × $La(thd)_3$, 2 × $Sr(thd)_2$, 3 × $Co(acac)_3$] which yields the metal stoichiometry of (0.3-0.4)La-(0.6-0.7)Sr-Co for the films for our further detailed studies. The precursor deposition cycles were mixed according to Fig. 4, to spread the different metal atoms as evenly as possible in the growing film. Using this supercycle scheme, a thickness series was made from 100 to 300 supercycles to evaluate the linearity of the growth rate, as shown in Fig. 5. The metal composition of these films was (0.23-0.30)La-(0.67-0.72)Sr-Co. Quite remarkably for a quaternary deposition process, the elemental uniformity was observed to be relatively good and insensitive to the position of the substrate in the reactor chamber. Even in the worst sample the La:Co ratio in the 100 supercycle deposition

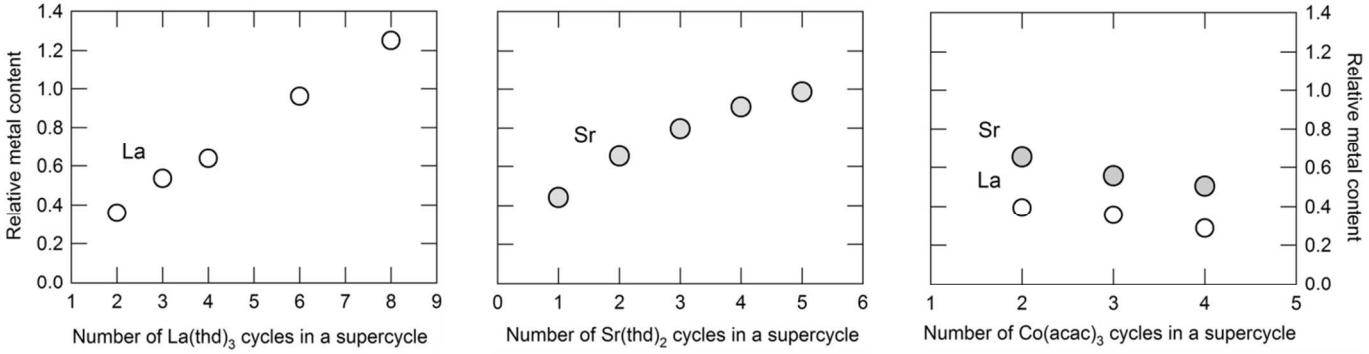

Fig. 3 Relative metal compositions of La (○) and Sr (●) to Co (set to 1) in the quaternary La-Sr-Co-O system, where the number of cycles for one precursor was increased gradually in the supercycle, while the cycle numbers for the other two precursors were kept the same.

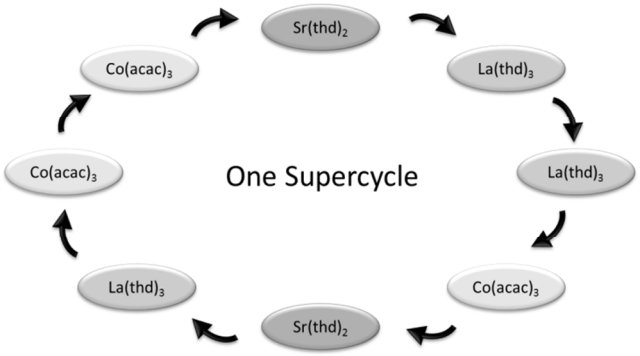

Fig. 4 One supercycle for depositing $(La_{0.3}Sr_{0.7})CoO_{3-\delta}$ films. Each black arrow represents 1.5 s N_2 purge + 3.0 s O_3 pulse + 2.5 s N_2 purge.

was 0.23 when the substrate was placed near the precursor inlet, while being 0.27 in the back of the chamber in the same deposition run, the Sr content being 0.69 and 0.71, respectively. The growth mode was also insensitive to the choice of the substrate material as no differences in thickness or cation stoichiometry were observed between films grown on borosilicate and silicon substrates. The film quality can be further confirmed from the XRR patterns,[30] shown in Fig. 5. For example, the film density seems to slightly increase with increasing film thickness, as indicated by the tiny increase in the critical angle. The interface roughness (inversely seen from the height of the oscillation amplitude) apparently slowly increases with increasing film thickness, while the surface roughness (evaluated from the decay of intensity) remains unchanged, indicating good film growth thorough the ALD process.

All the as-deposited 0.3La-0.7Sr-Co-O films were amorphous, and thus a post-deposition annealing was needed to achieve the perovskite type structure. We carried out these post-deposition heat treatments under two different atmospheres relevant to the SOFC cathode performance, that is, in Airgas (= 20 % O_2 + 80 % N_2) and 100% O_2. The films were kept at 500–900 °C for 15 min before cooling down; GIXRD patterns measured for the films immediately after the cooling are shown in Fig. 6. The films begin to crystallize at *ca*. 600 °C, and while the crystallinity at 800 °C is the best of the series, tiny peaks due to a Co_3O_4 impurity are already seen. Thus the optimal annealing temperature range is 700–750 °C. Additionally, although not shown in the figures, at 900 °C the films were found to decompose into corresponding binary oxides. Note

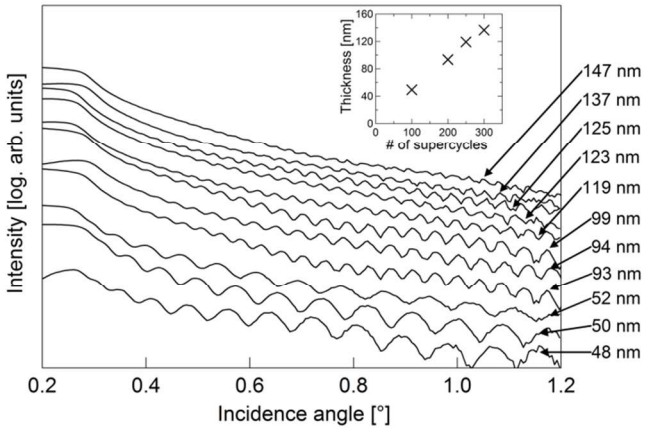

Fig. 5 XRR patterns of the amorphous films. **Inset**: The La-Sr-Co-O film thickness *vs*. number of supercycles increases in a highly linear manner.

that the GIXRD patterns were identical despite the atmosphere, thus only one pattern *per* temperature is shown in Fig. 6.

Figure 6 shows also the FTIR spectra recorded after each post-deposition annealing step for a single 125 nm thick film, revealing the carbonyl group from the $SrCO_3$ impurity[21] in the as-deposited and some post-annealed films. As the thin film crystallization to $(La_{0.3}Sr_{0.7})CoO_{3-\delta}$ evolves, the carbonyl group peak at *ca*. 1440 cm^{-1} diminishes, as expected. Similarly the evolution of the XRR pattern is presented with rising annealing temperature, showing the surface morphology changes associated with the crystallization process. The 600 °C, 700 °C and 800 °C post-annealed samples show an increasing decline in the intensity right after the critical angle, which is related to enhanced surface roughness. The increasing critical angle is apparently due an increasing density of the sample when it is crystallized.

Finally we carried out a test deposition to fabricate a $(La_{0.7}Sr_{0.3})CoO_{3-\delta}$ film, which was then annealed at 700 °C, see the GIXRD pattern in Fig. 6 (left). According to van Doorn *et al*.[31] the structure for this composition should be rhombohedral, while $(La_{0.3}Sr_{0.7})CoO_{3-\delta}$ is of near-perfect cubic symmetry. With GIXRD it is impossible to argue about crystal structure details; however, comparing to the PDF database (cubic $La_{0.3}Sr_{0.7}CoO_3$: 00-048-0137 and rhombohedral $La_{0.7}Sr_{0.3}CoO_3$: 04-013-1001), the peak intensity differences for the cubic and rhombohedral phases are seen mostly in the 2θ ranges of 23.2-23.5° and 47.4-48.1°, and it looks likely that the structures here are cubic $La_{0.3}Sr_{0.7}CoO_{3-\delta}$ and rhombohedral $La_{0.7}Sr_{0.3}CoO_{3-\delta}$. We also checked the lattice parameters from the peak positions to confirm that they were essentially equal to the PDF database values. Here we should emphasize that the crystal structures may also be affected by the small variations in the oxygen contents of the films, *i.e*. the δ parameter. Moreover, the ion conduction properties are likely to depend on the oxygen stoichiometry. Unfortunately it is highly challenging to experimentally detect such tiny variations in oxygen contents in thin-film samples.

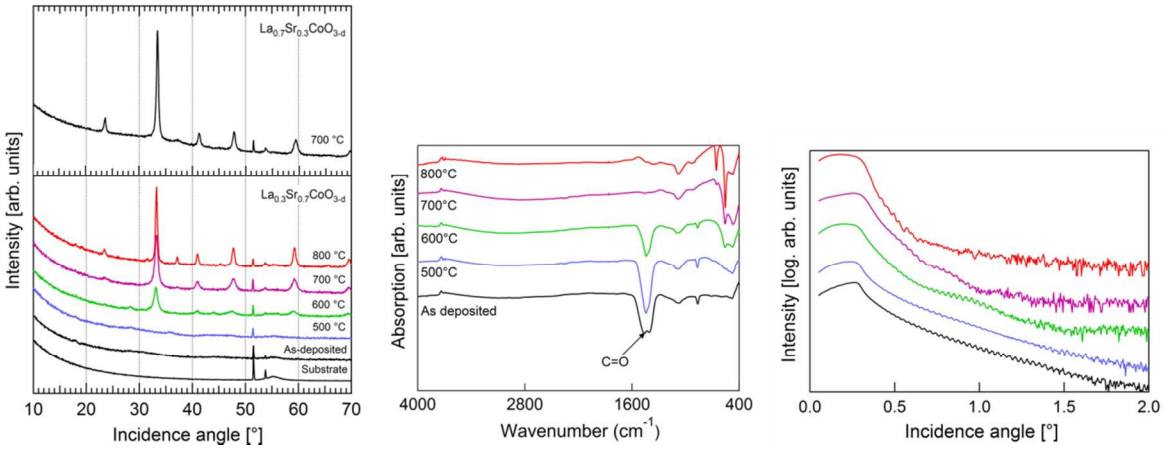

Fig. 6 Left above, GIXRD patterns for $(La_{0.7}Sr_{0.3})CoO_{3-\delta}$ thin film post-annealed at 700 °C. Below: GIXRD patterns for $(La_{0.3}Sr_{0.7})CoO_{3-\delta}$ thin films post-annealed at various temperatures, as-deposited film and the silicon substrate. In the middle and right figure, FT-IR and XRR analyses are shown for the post-annealed $(La_{0.3}Sr_{0.7})CoO_{3-\delta}$ thin films. Color online.

Conclusion

We have developed a promising new ALD process for the fabrication of high-quality $(La_{1-x}Sr_x)CoO_{3-\delta}$ thin films in a well-controlled manner within a wide composition range of $0.3 < x < 0.7$. Our work provides a highly positive indication that the ALD technology indeed can be extended to more complex film compositions. We moreover foresee that this particular fabrication process has true potential to be employed in future applications such as IT-SOFCs, in particular since an ALD process based on self-saturated surface reactions fundamentally allows the use of complex/nanostructured substrates with large surface areas. In the IT-SOFC technology the importance of using large-area substrates arises from the widely accepted fact that the IT-SOFC efficiency is currently limited by cathode performance issues related to film thickness and number of reactive sites (= surface area). Our post-deposition annealed crystalline $(La_{1-x}Sr_x)CoO_{3-\delta}$ thin films showed enhanced surface roughness and thus increased surface area even without employing a nanostructured substrate which should also be advantageous in SOFC cathode applications.

Acknowledgement

Mr. Hannu Revitzer is acknowledged for carrying out the ICP-OES measurements.

Notes and references

[a] Laboratory of Inorganic Chemistry, Department of Chemistry, Aalto University, P.O. Box 16100, FI-00076 AALTO, Espoo, Finland.
*E-mail: maarit.karppinen@aalto.fi; Fax: +358 9 462 73; Tel: +358 50 384 1726

1 C. Sun, R. Hui, and J. Roller, *J. Solid State Electrochem.*, 2009, **14**, 1125–1144.
2 A. J. Jacobson, *Chem. Mater.*, 2010, **22**, 660–674.
3 M. Prestat, A. Infortuna, S. Korrodi, S. Rey-Mermet, P. Muralt, and L. J. Gauckler, *J. Electroceramics*, 2007, **18**, 111–120.
4 A. Endo, S. Wada, C. Wen, H. Komlyama, and K. Yamada, *J. Electrochem. Soc.*, 1998, **145**, 1997–1999.
5 C. Peters, A. Weber, and E. Ivers-Tiffée, *J. Electrochem. Soc.*, 2008, **155**, B730.
6 S. Wang, J. Yoon, G. Kim, D. Huang, H. Wang, and A. J. Jacobson, *Chem. Mater.*, 2010, **22**, 776–782.
7 A. Mineshige, M. Kobune, S. Fujii, Z. Ogumi, and M. Inaba, *J. Solid State Chem.*, 1999, **142**, 374–381.
8 K. Iwasaki, T. Ito, T. Nagasaki, Y. Arita, M. Yoshino, and T. Matsui, *J. Solid State Chem.*, 2008, **181**, 3145–3150.
9 H. Kozuka, H. Yamada, T. Hishida, K. Yamagiwa, K. Ohbayashi, and K. Koumoto, *J. Mater. Chem.*, 2012, **22**, 20217.
10 S. M. George, *Chem. Rev.*, 2010, **110**, 111–31.
11 J. Lybeck, M. Valkeapää, S. Shibasaki, I. Terasaki, H. Yamauchi, and M. Karppinen, *Chem. Mater.*, 2010, **22**, 5900–5904.
12 K. Uusi-Esko and M. Karppinen, *Chem. Mater.*, 2011, **3**, 1835–1840.
13 M. Putkonen, T. Sajavaara, J. Niinistö, L.-S. Johansson, and L. Niinistö, *J. Mater. Chem.*, 2002, **12**, 442–448.
14 J. Shim, C.-C. Chao, H. Huang, and F. Prinz, *Chem. Mater.*, 2007, 3850–3854.

15 E. Gourba, A. Ringuede, M. Cassir, A. Billard, J. Päiväsaari, J. Niinistö, M. Putkonen, and L. Niinistö, *Ionics*, 2003, **9**, 15–20.
16 E. Ahvenniemi, M. Matvejeff, and M. Karppinen, *Appl. Surf. Sci.*, 2014, **320**, 838–842.
17 H. Seim, M. Nieminen, L. Niinisto, and H. Fjellvag, *Appl. Surf. Sci.*, 1997, **112**, 243–250.
18 O. Nilsen, M. Peussa, and H. Fjellvåg, *J. Mater. Chem.*, 1999, 1781–1784.
19 K. Uusi-Esko, E.-L. Rautama, M. Laitinen, T. Sajavaara, and M. Karppinen, *Chem. Mater.*, 2010, **22**, 6297–6300
20 O. Nilsen, E. Rauwel, H. Fjellvåg, and A. Kjekshus, *J. Mater. Chem.*, 2007, **17**, 1466.
21 M. Lie, O. Nilsen, H. Fjellvåg, and A. Kjekshus, *Dalton Trans.*, 2009, 481–489.
22 T. P. Holme, C. Lee, and F. B. Prinz, *Solid State Ionics*, 2008, **179**, 1540–1544.
23 E. V. Tsipis and V. V. Kharton, *J. Solid State Electrochem.*, 2008, **12**, 1367–1391.
24 C. H. Chen, H. J. M. Bouwmeester, R. H. E. van Doorn, H. Kruidhof, and A. J. Burggraaf, *Solid State Ionics*, 1997, **98**, 7–13.
25 D. J. L. Brett, A. Atkinson, N. P. Brandon, and S. J. Skinner, *Chem. Soc. Rev.*, 2008, **37**, 1568–78.
26 R. H. E. van Doorn, H. Kruidhof, A. Nijmeijer, L. Winnubst, and A. J. Burggraaf, *J. Mater. Chem.*, 1998, **8**, 2109–2112.
27 R. H. E. van Doorn, I. C. Fullarton, R. A. de Souza, J. A. Kilner, H. J. M. Bouwmeester, and A. J. Burggraaf, *Solid State Ionics*, 1997, **96**, 1–7.
28 V. V. Kharton, E. V. Tsipis, A. A. Yaremchenko, I. P. Marozau, A. P. Viskup, J. R. Frade, and E. N. Naumovich, *Mater. Sci. Eng. B*, 2006, **134**, 80–88.
29 G. Hammond, D. Nonhebel, and C. Wu, *Inorg. Chem.*, 1963, **2**, 8–11.
30 M. Yasaka, *Rigaku J.*, 2010, **26**, 1–9.
31 R. H. E. van Doorn and A. J. Burggraaf, *Solid State Ionics*, 2000, 128, 65–78.

An atomic layer deposition (ALD) process has been developed to fabricate quaternary oxide $(La,Sr)CoO_3$ thin films in a well-controlled manner within a wide composition range. A post-deposition treatment crystallizes the films in a perovskite structure. The new process has true potential to be employed in future applications like IT-SOFCs.